

## Scientific workflows for MHD stability chain analysis of tokamak plasmas

R. Coelho<sup>[1]</sup>, A. Merle<sup>[2]</sup>, G. Vlad<sup>[3]</sup>, D. Yadikin<sup>[4]</sup>, M. Owsiak<sup>[5]</sup>, O. Sauter<sup>[2]</sup>, I. Chapman<sup>[6]</sup>, M. Dunne<sup>[7]</sup>, P. Buratti<sup>[3]</sup> and JET contributors<sup>&</sup> and ASDEX Upgrade Team and the EU-IM Team<sup>\*</sup>

EUROfusion Consortium, JET, Culham Science Centre, Abingdon, OX14 3DB, UK

- [1] Instituto de Plasmas e Fusão Nuclear, Instituto Superior Técnico, Universidade de Lisboa, 1049-001 Lisboa, Portugal
- [2] École Polytechnique Fédérale de Lausanne (EPFL), Centre de Recherches en Physique des Plasmas (CRPP), CH-1015 Lausanne, Switzerland
- [3] ENEA for EUROfusion, via E. Fermi 45, 00044 Frascati (Roma), Italy
- [4] Department of Earth and Space Sciences, Chalmers University of Technology, SE-41296 Göteborg, Sweden
- [5] Poznan Supercomputing and Networking Center, IChB PAS, Noskowskiego 12/14, Poznan, Poland
- [6] Culham Centre for Fusion Energy, Culham Science Centre, Abingdon, Oxfordshire, OX14 3DB, UK
- [7] Max Planck Institute for Plasma Physics, Boltzmannstr. 2, 85748 Garching, Germany

### I – Introduction

The onset of MHD activity in present tokamak plasmas plays a detrimental role in the discharge performance and operational limits. The characterisation of the MHD modes observed is often assisted by predictions from linear MHD codes. Estimation of the MHD stability boundaries in operational plasma scenarios foreseen for ITER and future devices such as DEMO is also crucial. Building confidence on MHD code suite predictions calls for the benchmark of the high-resolution MHD equilibrium and stability solvers involved, a task that is greatly facilitated when all codes share the same physics and machine data ontology and methods for reading and writing the data, as in the European Integrated Modelling (EU-IM) framework [1], presently maintained by the EUROfusion Code Development Work Package. Under its auspices, a Kepler [2] scientific workflow for the analysis of MHD activity in tokamak plasmas was developed (see Figure 1), pluggable to equilibrium reconstruction or discharge simulator workflows. A custom “actor” extracts, from full domain

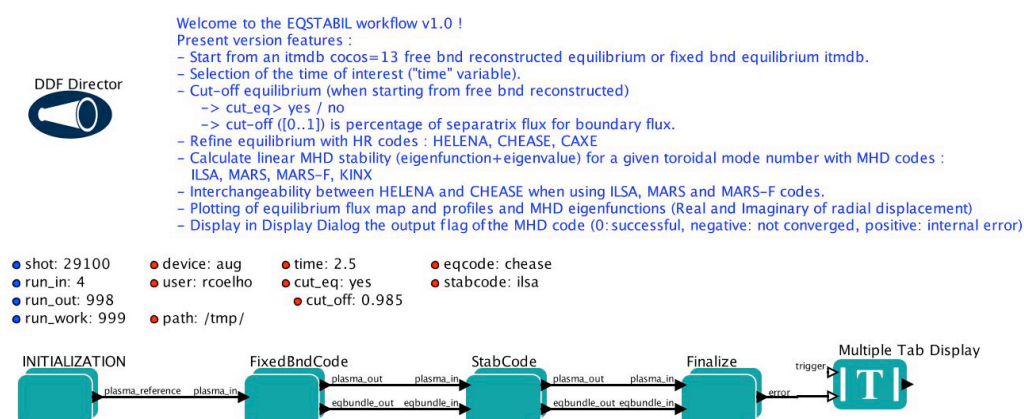


Figure 1 – Kepler workflow for equilibrium and MHD stability of tokamak discharges

\* See <http://www.euro-fusionscipub.org/eu-im>

& See the Appendix of F. Romanelli et al., Proceedings of the 25th IAEA Fusion Energy Conference 2014, Saint Petersburg, Russia

equilibrium with a separatrix, a nested closed flux surface equilibrium with plasma boundary flux at selected fraction of the separatrix flux. The workflow presently includes HELENA [3], CHEASE [4] and CAXE [5] equilibrium codes and ILSA [6], MARS [7], MARS-F [8] and KINX [5] linear MHD stability codes. Modular approach allows equilibrium and stability codes to be fully interchangeable for compatible equilibrium metrics e.g. ILSA/MARS/MARS-F, compatible with the jacobian  $J \propto R^2$  straight field line coordinate system provided by CHEASE/HELENA. KINX, capable of addressing plasmas with separatrix, is limited to using a custom made quasi-polar quadrangular grid adapted to nested magnetic surfaces provided by CAXE.

## II – Benchmark results

Synthetic equilibria (circular and up-down symmetric elongated with equidistant radial meshes) and experimental (JET #77877  $t=46.2s$  and AUG #29100  $t=1.62$ ) equilibria unstable to either  $n=1$  internal or global ideal kink modes were used. The tests focused on the growth rate ( $\gamma$ ) convergence with poloidal harmonic spectra (except for KINX since it is not a spectral code) and with the radial/poloidal mesh size. For the poloidal harmonic ( $m$ ) convergence, alternate convergence in upper/lower limits was done, starting from a relatively small range  $m=[m_1, m_2]$ , until a relative error threshold ( $\sim 10^{-6}$ ) in the real part of  $\gamma$  was reached. The converged setting of each code was then used for the radial/poloidal grid size scan and verify the expected  $1/N_{\text{grid}}^2$  scaling ( $N_{\text{grid}}$  being the number of grid points). ILSA runs were always carried out using the MISHKA-1 code kernel. The circular synthetic equilibria ( $N_{\psi}=200$ ,  $N_{\theta}=128$ ) had a perfect conducting wall far away (no-wall limit) from the plasma boundary i.e.  $R_{\text{ext}}=(R_{\text{wall}}-R_{\text{geo}})/a=3.5$ , while the elongated equilibria ( $N_{\psi}=200$ ,  $N_{\theta}=128$ ) had the wall at the plasma boundary. The agreement between all codes in the converged  $\gamma$  is very good, with a normalised converged standard deviation in  $\gamma$  ( $g_N$ ) of order  $\sim [0.3-1.8]\%$ , as observed from Table I, although poloidal spectra range becomes noticeably larger in ILSA for elongated plasmas. Conversely,  $m$ -range in MARS/MARS-F may be reduced when using equal-arc length coordinate system provided by CHEASE (not used in scaling exercises).

Code	Circular			Elongated		
	m1	m2	Growthrate	m1	m2	Growthrate
ILSA/CHEASE	-3	13	5.65903380E-02	-30	40	6.94658070E-02
ILSA/HELENA	-	-	-	-28	44	6.94541270E-02
MARS/CHEASE	-2	12	5.62763000E-02	-21	39	6.96735000E-02
MARSF/CHEASE	-6	10	5.62715461E-02	-14	30	6.98718153E-02
CAXE/KINX	-64	64	5.84452758E-02	-64	64	6.98699193E-02

Table I – Poloidal spectra convergence for the synthetic equilibria cases.

The radial profile and normalised intensity (integral of eigenfunction squared over radial flux coordinate) of the dominant harmonics of the radial velocity eigenfunction show an excellent match among all codes. Agreement of growth rate scaling with radial/poloidal grid size ( $1/N^2$ ) was verified for radial grid size  $N > 200$  and poloidal grid sizes covering the poloidal spectra. As anticipated,  $g_N$  drops/saturates as grid size is increased. For the equilibria of JET ( $B_T \sim 2.66$ ,  $I_p \sim 1.7$  MA,  $\beta_N \sim 2.67$ ,  $N_\psi = 300$ ,  $N_\theta = 256$ ) and AUG ( $B_T \sim 2.4$ ,  $I_p \sim 0.97$  MA,  $\beta_N \sim 2.55$ ,  $N_\psi = 250$ ,  $N_\theta = 512$ ), there is a wider scattering in converged  $\gamma$  ( $g_N \sim 3.7\%$  for JET and  $g_N \sim 0.9\%$  for AUG) as indicated in Table II. Equilibrium and stability were done with packed radial meshes around rational surfaces and at the plasma boundary and uniform in vacuum. The conducting wall was placed at  $R_{\text{ext}} = 1.3$  for JET (close to marginal stability –  $R_{\text{ext}} \sim 1.08$ ) and 1.5 for AUG.

JET (#77877)				AUG (#29100)		
Code	m1	m2	Growthrate	m1	m2	Growthrate
ILSA/CHEASE	-21	67	5.30770720E-03	-46	72	3.05979620E-02
ILSA/HELENA	-29	67	5.49354640E-03	-	-	-
MARS/CHEASE	-19	38	5.10869000E-03	-20	35	3.01958903E-02
MARSF/CHEASE	-9	33	5.30046053E-03	-14	30	3.03251268E-02
CAXE/KINX	-128	128	5.62557314E-03	-256	256	3.06957636E-02

Table II – Poloidal spectra convergence for the JET/AUG equilibria cases.

The grid scaling tests for the JET and AUG cases are shown in Figure 2 and evidence the different convergence trends of the several codes and the sensitivity to different equilibrium solvers and/or radial meshes (packing is done differently in CHEASE/HELENA/CAXE). Convergence for JET equilibrium is challenged by the proximity to marginal stability and thus to the particular meshing used in the equilibrium and MHD codes. Radial velocity eigenfunctions and normalised intensities are in good agreement and, as anticipated, show slight differences ( $< 5\%$ ) depending on the equilibrium code. The rougher grid scaling observed with ILSA when compared to the other codes is also reflected on the eigenfunctions and normalised intensities (closest match between MARS, MARS-F and KINX).

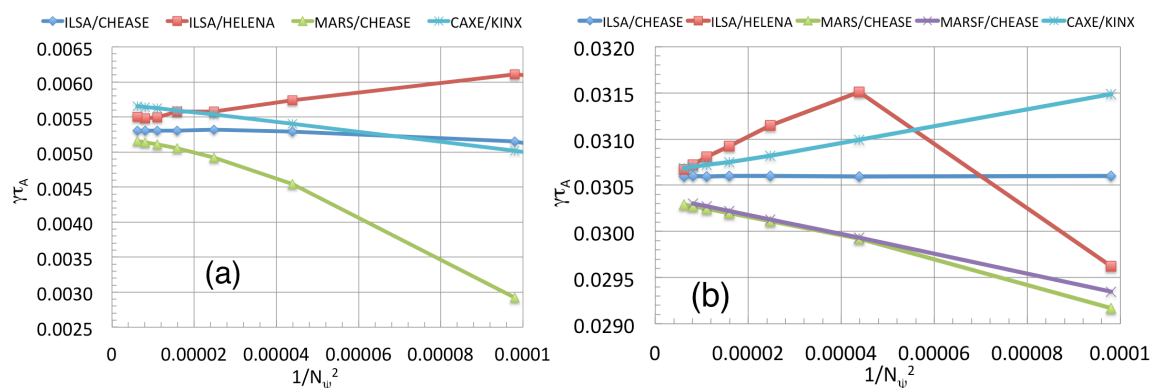


Figure 2 – Radial grid scaling of  $n=1$  normalised growth rate for JET (a) and AUG (b) equilibrium.

The dependence of  $\gamma$  on  $R_{\text{ext}}$  was also probed for JET and AUG plasmas (same code parameters as used for the poloidal convergence) and the marginal stability threshold yielded similar results on all codes, with some differences observed closer to the no-wall limit, as indicated in Figure 3, in particular for the JET case. Both plasmas have similar elongation ( $\sim 1.7$ ) but triangularity is 25% higher in JET and AUG plasma has no upper triangularity thus the JET case results might indicate a higher sensitivity of the codes to the equilibrium used.

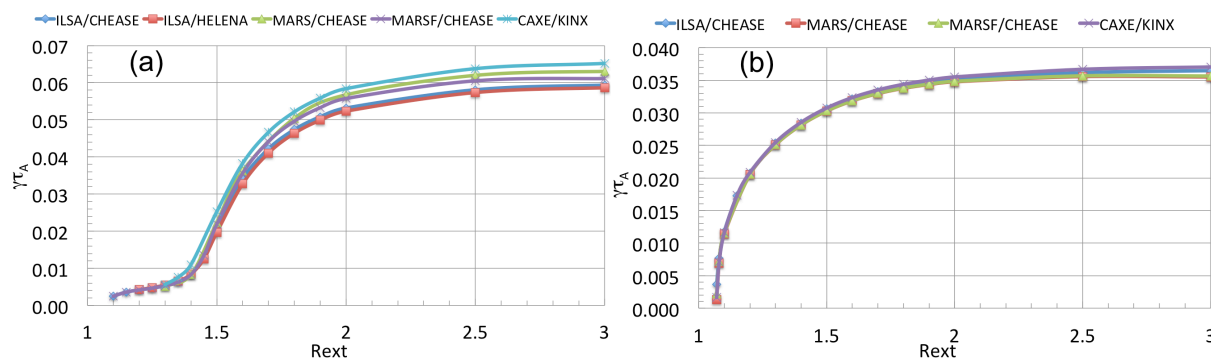


Figure 3 – Growth rate scaling of  $n=1$  mode with wall position for JET (a) and AUG (b) equilibrium

## IV – Conclusions

A benchmark of the MHD stability codes installed on the EU-IM modelling platform was performed, addressing code convergence with poloidal harmonics, grid resolution and growthrate dependence on radial location of a conformal conducting wall. Synthetic (circular and elongated) and experimental (JET #77877 and AUG #29100) equilibria were used to study  $n=1$  internal and global kink unstable modes. The agreement on convergence tests, scalings and eigenfunctions/spectra is quite good overall with the experimental JET case showing the largest deviations among codes (though  $g_N$  is limited to less than 5%).

## Acknowledgements

This work has been carried out within the framework of the EUROfusion Consortium and has received funding from the Euratom research and training programme 2014-2018 under grant agreement No 633053. IST activities also received financial support from “Fundação para a Ciência e Tecnologia” through project UID/FIS/50010/2013. The views and opinions expressed herein do not necessarily reflect those of the European Commission.

## References

- [1] F. Imbeaux et al *Comp. Phys. Comm.* **181**(6):987-998, 2010
- [2] <https://kepler-project.org/>
- [3] G.T.A. Huysmans et al., *Proceedings of the CP90-Conference on Computational Physics*, World Scientific Publishing Co.,1991, p. 371
- [4] H. Lütjens et al., *Comp. Phys. Comm.* **97** (1996) 219
- [5] Degtyarev et al., *Comp. Phys. Comm.* **103** (1997)
- [6] C. Konz et al., *Scientific Workflows for the Linear MHD Stability Analysis Chain*, 37th EPS Conference, Dublin 2010
- [7] A. Bondeson et al., *Phys. Fluids* **B 4** (1992) 1889
- [8] Y. Q. Liu et al., *Phys. Plasmas* **7** (2000) 3681